Available online at www.sciencedirect.com

ScienceDirect

Procedia CIRP 100 (2021) 169–174

www.elsevier.com/locate/procedia

31st CIRP Design Conference 2021 (CIRP Design 2021)

Production-oriented design of electric traction drives with hairpin winding

Prof. Dr.-Ing. Jürgen Fleischer[a,]*, Ludwig Hausmann[a], Felix Wirth[a]

[a]*Karlsruhe Institute of Technology, wbk Institute of Production Science, Kaiserstraße 12, 76131 Karlsruhe, Germany*

* Corresponding author. Tel.: +49-721-608-44009; fax: +49-721-608-45005. *E-mail address:* juergen.fleischer@kit.edu

Abstract

In recent years, the manufacturing of stators by hairpin technology has proven its ability to fulfill the requirements on quality, productivity and robustness of traction drive applications in automotive industry. However, the uncertainty and necessity of rapid product development despite fuzzy target systems still cause that processes, machines and equipment – as well as the electric design – are often in an imperfect prototype stage at the start of production ramp-up. Due to the complex interdependencies between the stator components in combination with a high sensitivity of the overall process reliability to minor adjustments of stator design features, possible production-related weaknesses in design are often recognized first in the prototype stage of the production system. In order to reduce the economic risk resulting from these volatile technological conditions, production-oriented design based on numerical simulation methods can be applied from the beginning of product development. Therefore, several techniques for numerical process modeling are presented in this paper as possibilities to consider manufacturing constraints in an early stage of product development. For this purpose, the influence of wire dimensions on the forming process of hairpin coils is investigated using the example of rotary bending as well as the twisting process of a full stator by finite element simulations. Furthermore, a numerical approach to investigate the influence of heat input during laser welding of hairpin coils on the required stripping length is introduced.

Keywords: Electric drives manufacturing; Hairpin technology; Production-oriented design; Numerical process simulation

1. Introduction and motivation

Mainly driven by strict legislation as well as the growing trend for sustainable and climate-neutral mobility, an extensive transformation from combustion-engined power trains to electric mobility is expected within this decade. This fundamental change in drive technology already leads to a high demand for powerful and efficient electric traction drives in automotive industry. The manufacturing of electric drives for traction applications requires production technologies with high productivity, process reliability and fault tolerance to enable cost-efficient and competitive production with minimum waste [1]. Moreover, enhanced automotive requirements regarding power density, efficient operating behavior over a wide range of speed, noise generation and robustness against environmental influences cause novel challenges in both product development and production engineering in comparison to classical industrial applications [2]. As a result of continuous improvements along the process chain in recent years, the hairpin technology has proven its ability to fulfill the requirements on stator manufacturing in automotive serial production. However, the competitive need for a minimum time to market as well as dynamic developments in drive technology still cause that processes, machines and equipment as well as the electric design are often in an imperfect prototype stage at the start of production ramp-up. Due to the complex interdependencies between product characteristics and manufacturing processes, production-related weaknesses in design are often recognized first in the prototype stage of the production system. In order to reduce the economic risk resulting from these volatile conditions by production-oriented and thus cost-efficient stator design, numerical simulation methods can be applied from the beginning of product development. [3] Therefore, several

2212-8271
10.1016/j.procir.2021.05.080

numerical techniques are introduced in this paper to show the potential of process simulations for considering manufacturing constraints in an early stage of product development. In this context, the influences of wire dimensions and tooling parameters on the forming process of hairpin coils are analyzed using the example of rotary bending as well as the twisting process of a full stator by finite element simulations. Furthermore, a numerical approach to investigate the influence of process-related heat input during laser welding of hairpin coils on the required stripping length is introduced.

2. State of the art

Due to its high relevance for industrial electric drives production, the hairpin technology has been analyzed in detail by several research groups, e. g. by Riedel et al. in 2018 [4]. In general, the simplified process chain consists of five subsequent steps: shaping (straightening, stripping, cutting and bending) of enameled rectangular copper wire, joining (slot lining, composing and inserting) of hairpin coils and lamination stacks, widening, twisting and contacting (masking, cutting and welding) of the inserted coils as well as a concluding impregnating and insulating of the stator with hairpin winding. The industrial process chain for manufacturing of stators by hairpin technology is visualized in Fig. 1.

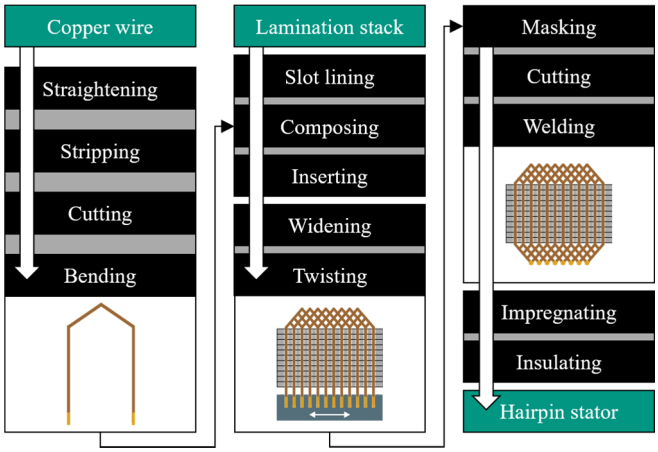

Fig. 1. Process chain for manufacturing of stators with hairpin winding.

In addition, Gläßel and Pinhal et al. analyzed the effects of manufacturing influences, as changes in the electric resistance of hairpin coils by bending and contacting processes, on the performance of an electric machine by experiments and drive cycle simulations [5]. Besides, a summary of scientific investigations on the design of stators with rectangular wire winding was given by Zhao et al. in [6]. Furthermore, coherences between design, manufacturing and performance of electric drives were systematically identified and described in a literature study by Halwas et al. in [2] and [7].

Within the scope of hairpin technology, Weigelt et al. described quality characteristics of hairpin coils by explicit finite element analyses of the elementary forming operations three-point and die bending [8]. Moreover, Wirth et al. analyzed the influences of wire tolerances on a sequence of tool-bound as well as kinematic hairpin bending operations by explicit and implicit finite element simulations, considering springback effects [3,9]. The hairpin welding process was studied by Gläßel using finite element simulations to determine the influence of feed rate, laser power and welding time on the surface temperature [10]. An overview about the most important modeling approaches for electric drives production in general is given in [11].

3. Approach and methodology

In the following section, simulation techniques for the assistance of the design process of hairpin stators under consideration of production-related constraints are presented. Models for the three core processes hairpin bending, twisting and welding are introduced and used to perform parameter studies to determine the correlations between design characteristics and process parameters.

4. Numerical study on hairpin bending processes

4.1. Modeling approach and parametrization

In order to analyze the influence of forming effects resulting from rotary bending on the cross-section of hairpin coils, a fully parametrized explicit finite element simulation model was built in Abaqus CAE 2019. The elastic-plastic forming properties of the enameled copper wire were described by experimental data acquired by uniaxial tensile tests as introduced in [9]. Due to high strains, Hockett-Sherby hardening was applied to extrapolate the experimental flow curve. Based on convergence studies, the wire was discretized by a structured mesh with a total number of 64 elements in cross-section and an axial element length of 0.5 mm within the forming zone. Therefore, a total number in between 8092 to 15572 linear volume elements of type C3D8R was used for geometrical discretization resulting from different wire lengths.

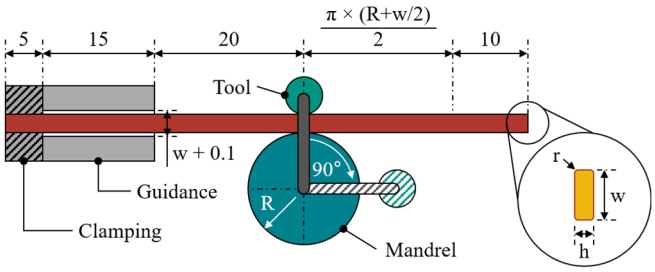

Fig. 2. Geometrical set-up of the numerical rotary bending simulation model.

As shown in previous Fig. 2, the wire was clamped over a length of 5 mm by geometrical boundary conditions and guided on a length of 15 mm with clearance of 0.1 mm. Because of the high stiffness of the tools in comparison to the enameled copper wire, the guidance, the mandrel as well as the bending tool were modeled as rigid bodies. For modeling the contact of wire and tools, a conventional penalty contact and a friction coefficient of 0.1 were chosen. The simulation time was set to 0.5 s according to experimental bending operations without time scaling. Due to the quasi-static characteristic of the bending operation, a global mass scaling factor of 32 was rated as acceptable to minimize the calculation effort. After the explicit dynamic forming simulation a static implicit analysis of 1 s was implemented to model the subsequent springback effects.

4.2. Numerical parameter study

In total, seven parameter levels in wire cross-section as well as six parameter levels of bending radii were varied in a full factorial parameter study as shown in Table 1. As a consequence of the ongoing trend for maximum copper fill factors, the wire edge radii were set to a constant value of 0.25 mm. Hence, the changes in wire cross-section caused by the rotary bending operation, visualized in Fig. 2, were analyzed by a total number 7 × 6 = 42 simulations.

Table 1. Characteristic parameters and parameter levels in numerical analysis.

Parameter	Parameter levels in mm						
Wire width (w)	2		3		4		5
Wire height (h)	1.5		2		2.5		3
Wire radius (r)				0.25			
Wire type (w × h)	2×1.5	3×1.5	3×2	4×2	4×2.5	5×2.5	5×3
Bending radius (R)	5	7.5	10	15	20	40	

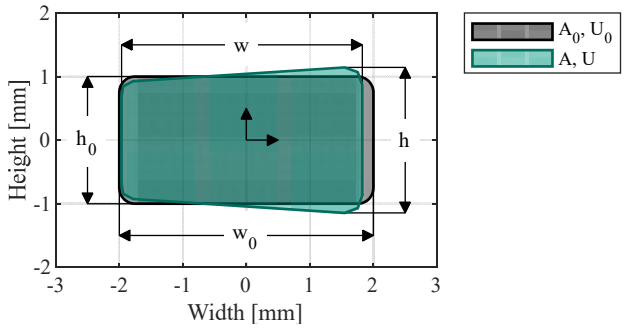

Fig. 3. Original (gray) and deformed (green) wire cross-section as well as characteristic geometry parameters in height and width direction using the example of 4 × 2 mm² cross-section and a bending radius of 5 mm.

As shown in Fig. 3, the rectangular wire cross-section is significantly influenced by the bending operation in both dimensions and shape. Whereas the cross-sectional area is nearly constant due to the manner of the analyzed rotary bending process, the rectangular shape is transformed into a characteristic trapezoid. Based on this analysis, the surface specific changes in wire cross-section can be described by two aspect ratios in height and width as scalar variables. Hence, the 42 results of the numerical parameter study were evaluated at the center of forming zone, which corresponds to a bending angle of 45° after forming. The results referring to these analyses are visualized in Fig. 4 and indicate that the relative change in height is less significant than in width. Furthermore, the transformation in shape is more extensive at the inner than at the outer fiber of the wire in general. Besides, the relative changes in shape increase by rising width but decreasing height of the wire. In addition, an empirical function (1) was identified to describe the ratios in both height and width direction approximately:

$$f(w, h, R) = 1 + (a \cdot w + b \cdot h) / (R + c) \quad (1)$$

Hereby, the influence of rotary forming operation on the wire cross-section can be described by three parameters depending from material properties, friction conditions and the wire edge radius. In future, this knowledge can be used to extend automated tools for winding head optimization as introduced in [11]. This enhancement meets the rising need for considering realistic air gaps and leakage paths in insulation system design – especially against the background of high performance applications at 800 V or even higher operating voltage.

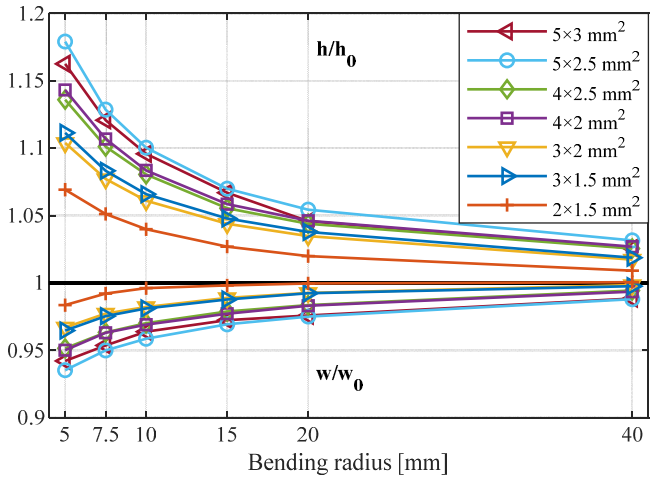

Fig. 4. Ratio of changes in height and width direction of the wire by rotary bending operations at different bending radii.

5. Numerical study on hairpin twisting processes

The hairpin twisting process is used to realize the wave-like winding pattern of hairpin stators by simultaneous forming of the free wire ends. In this process, usually several hundreds of wires are simultaneously interleaved against each other by a superposition of radial planar motion and axial compensation motion using a stator-specific tool set. Due to the small installation space, the non-linear motion as well as the number of interacting wires, the process is highly sensitive to the wire aspect ratio, the geometrical tolerances of the tooling and the motion control. Interdependencies between stator design parameters and the manufacturing process can only be determined experimentally at great expense, which makes the use of simulative methods very attractive in this context.

5.1. Modeling approach

The fully parameterized FE-model introduced in [11] was used to study the main influences on the twisting process focusing the wire elongation. The model, which is implemented in Abaqus CAE 2019, allows numerical studies on isolated parameters by selectively varying of geometric sizes in an explicit forming simulation. In order to take the material history as well as the springback effect into account, the widening step before the actual twisting process and the pull out of the twisting tool afterwards are also simulated.

5.2. Numerical parameter study

A full factorial parameter study with a total of 54 simulations was conducted by a variation of the wire cross-

section (3×1.5, 4×2, 5×2.5 mm^2), the radial and tangential tool gap (150/300, 100/200, 50/100 µm), the tool and support finger bending radius (2, 4, 6 mm) and the friction coefficient between wires and tools (0.15, 0.3); the general geometric model parameters are shown in Table 2. After the simulations, the main effects on the elongation of the wires are analyzed in Fig. 5. Depending on the parameter combination, the average wire elongation is about 0.7 to 1.7 % of the initial length, which is neither negligible for product design nor process control. Whereas the wire elongation increases significantly with increasing wire cross-section, the bending radius has only a minor influence. In general, knowledge about the dependencies of wire elongation can be used to derive both optimized tool concepts as well as initial process parameters, e. g. for axial compensation.

Table 2. Geometric parameters and parameter levels of the twisting model.

Parameter		Parameter	
Inner twist radius	85 mm	Wire radius	0.25 mm
Final twist angle	22.5°	Free wire length	70 mm
Overtwist angle	1°	Slot height	15 mm
Radial wire gap	0.15 mm	Twist tool height	20 mm
Paper margin	3 mm	Slot/tool distance	46 mm
Paper thickness		75/100/75 µm	
Radial widening wire #1 – #6		0, 0.75, 5.25, 6, 10.5, 11.25 mm	

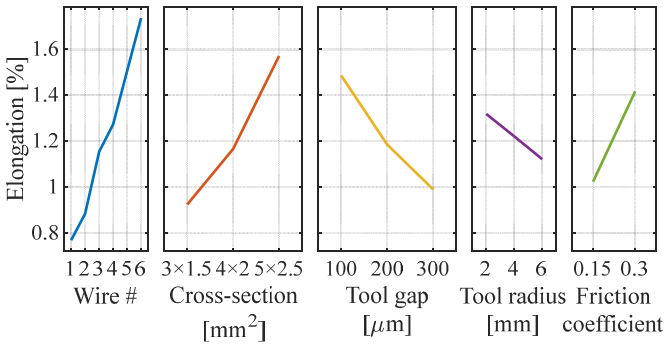

Fig. 5. Main effects of wire cross-section, tool gap, tool radius as well as friction between wire and tooling on the wire elongation.

Within the parameter study only one stator slot with six wires was simulated. However, if the exact geometric shape of the wires or the distances between the layers after twisting are of interest, this is not sufficient. Especially in stator designs with large wire cross-section ratio, stators with small inner diameters and compact winding heads often show a strong interaction between the individual layers. In order to analyze influences amongst the wires and strategies against wire torsion by simulations, Python scripts are used for automatic model creation, considering an arbitrary number of slots as well as optional radial support rings of different geometries. This enables to investigate the influence of design parameters on twisting processes at the beginning of product development and the design of twisting tools for series production. Considering that the production of a complete tool set usually takes 2–3 weeks, a prior evaluation of the concept can offer a significant advantage. Although finite element simulation models provide a comprehensive analysis of production processes, the high computational effort of large models, as shown in Fig. 6, makes them unsuitable for extensive parameter studies in some cases.

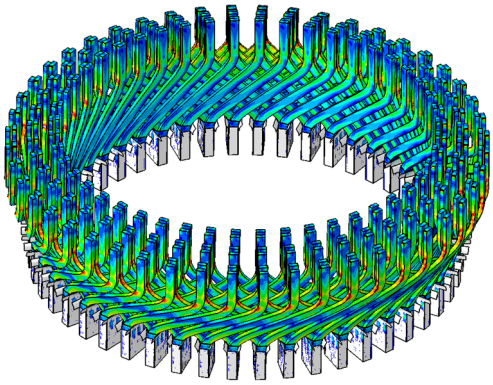

Fig. 6. Twisting simulation of a hairpin stator with 48 slots. Total computational time 52 hours on 40 cores.

6. Numerical study on hairpin welding processes

In the following section a new model-based approach is introduced to investigate the influence of process-related heat input during laser welding of hairpin coils on the required stripping length. The aim is not to represent the complex melting and solidification processes in the welding spot in detail, but to describe the relationship between energy input rate and stripping length to the resulting volume of the welding spot as well as the critical temperature for the wire insulation. The focus is on the reduced modeling of the three-dimensional heat transfer problem by a dimensional reduction. Assuming a constant temperature distribution over the wire cross-section, a one-dimensional substitute model for the simulation of heat transfer was implemented in the modeling language Simscape as part of MATLAB/Simulink due to the high thermal conductivity of copper.

6.1. Modeling approach and parametrization

The system model is divided into four main parts – the heat source, the stripped wire section above the tension masking, the stripped wire section within the tension masking and the insulated wire section of the winding head. The modeling of the wire under consideration of the thermal resistance, heat capacity as well as heat dissipation by convection and thermal radiation is shown in Fig. 7. To account for the temperature-dependent thermal conductivity coefficient of copper as determined in [12], a custom temperature-dependent resistor was implemented. Furthermore, the laser source has been modeled by a customized thermal heat source. This block enforces a certain heat flow between the environment and the outputs activated in the current time step, which is done by a predefined data table or a simplified welding strategy.

The only section that is not yet considered is the tension masking, which is crucial to the thermal behavior of the system. While the heat transfer could also be captured by an additional one-dimensional substitute circuit, the parametrization is not straightforward and can be ambitioned for complex geometries.

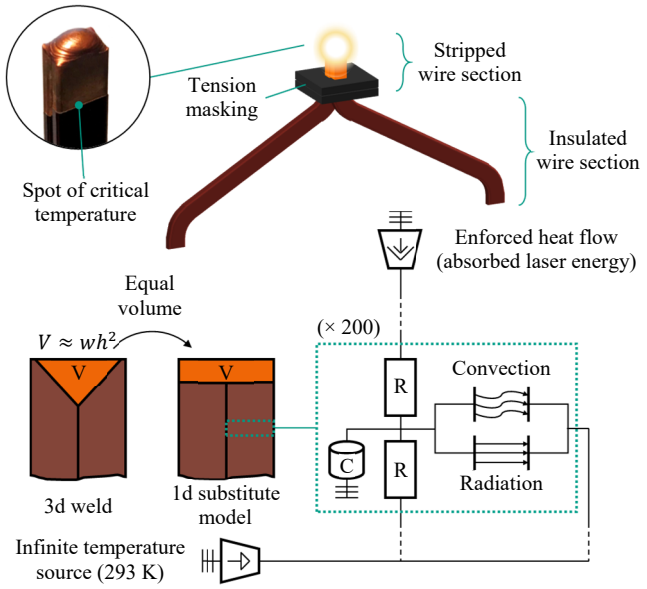

Fig. 7. Problem description and approach of the laser welding model.

For this reason a coupling of the Simscape model with a three-dimensional thermal FE-model was used, which allows to combine advantages of both the flexibility and computational efficiency of the thermal circuit modeling as well as the consideration of arbitrary complex geometries – at a neglectable modeling error. For this purpose an additional FE-model of the masking was created in addition to the Simscape model, using the MATLAB Partial Differential Equation Toolbox and based on flexible stl-file import. The coupling is realized by alternating between the two models within each time step, whereby the boundary conditions are kept constant within the contact zone. After calculating one step in time in the Simscape model, the temperature in the contact zone is averaged in area and time and subsequently enforced as constant boundary condition to the FE-model at the same time step. After taking the time step for the FE-model the heat flow over the contact surface is integrated and enforced by a controlled heat flow block in the Simscape model in the next time increment.

Table 3. Material-based input parameters of the laser welding model.

Parameter	
Copper density at 293 K	8.96 g/cm^3
Copper thermal conductivity at 293 K	385 W/(m·K)
Copper specific heat	390 J/(kg·K)
Copper heat of fusion	205 kJ/kg
Copper emissivity coefficient	0.25
Copper melting temperature	1356 K
Copper boiling temperature	2868 K
Steel density at 293 K	7.85 g/cm^3
Steel thermal conductivity at 293 K	80 W/(m·K)
Steel specific heat	460 J/(kg·K)
Heat-transfer coefficient	10 W/(m^2·K)
Thermal contact resistance copper-copper	4e^{-5} m^2·K/W
Thermal contact resistance copper-steel	1e^{-4} m^2·K/W

Unfortunately the heat flow absorbed by the masking highly depends on the thermal resistance of the contact zone, which is a function of the contact area and therefore influenced by the roughness of the interfaces as well as the applied contact pressure. For the roughness and pressure dependent thermal contact resistance between copper and different metals only few literature values are available. Hence, the physical behavior is better captured by calibration in a simplified experimental setup, e. g. by measuring the temperature history at the transition from the stripped wire to the insulated region once with and without masking. Nevertheless the influence of the masking can be well analyzed by varying the contact resistance over a wide region and can therefore be used to estimate worst and best case scenarios. In Table 3 the material parameters used for model-parametrization are summarized. The temperature dependent conductivity of copper was set according to [12].

6.2. Numerical parameter study

Two key parameters for the design of hairpin stators are the necessary stripping length and the resulting total length of the copper wire. Every millimeter of copper wire saved reduces the axial installation space, the ohmic coil resistance and of course material costs. However, the minimum achievable stripping length without damaging the wire insulation strongly depends on the welding process. In the following study, the modeling approach described before was used to determine these interdependences for the welding process of two wires by a wide variation of energy input rate, welding time and wire stripping length for three different wire cross-sections of 2×1, 3×1.5 and 4×2 mm^2. In addition, a tension masking of 5 mm thickness was included according to following Fig. 8.

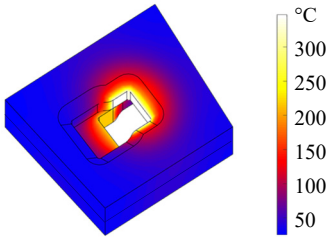

Fig. 8. Tension masking for the wire with cross-section of 3×1.5 mm^2.

For each wire cross-section about 80 simulations were carried out and the resulting welding depth and the maximum temperature at the stripping edge were evaluated. Afterwards, the results are summarized in contour diagrams, which are shown in Fig. 9. The diagrams were created by plotting the product of stripping length and maximum temperature in relation to an arbitrary temperature limit above the energy input rate and subsequent interpolation of the welding depth shown by the contour lines. The red line highlights the welding depth, which corresponds to the approximated volume of the weld spot as introduced in Fig. 7. Using the diagrams, the stator design parameters can be adapted to the characteristics of a particular welding system. First, the energy input rate is calculated by multiplying the laser output power by the average absorption coefficient corresponding to the wavelength of the laser. By intersecting the energy input rate with the target

welding depth, the combination of the necessary welding time as well as the shortest possible stripping length can be read from the diagram. The approach is not limited to model the welding of two wires and can be extended in order to evaluate the thermal heat distribution for more complex welding tasks or strategies considering surrounding mechanical components.

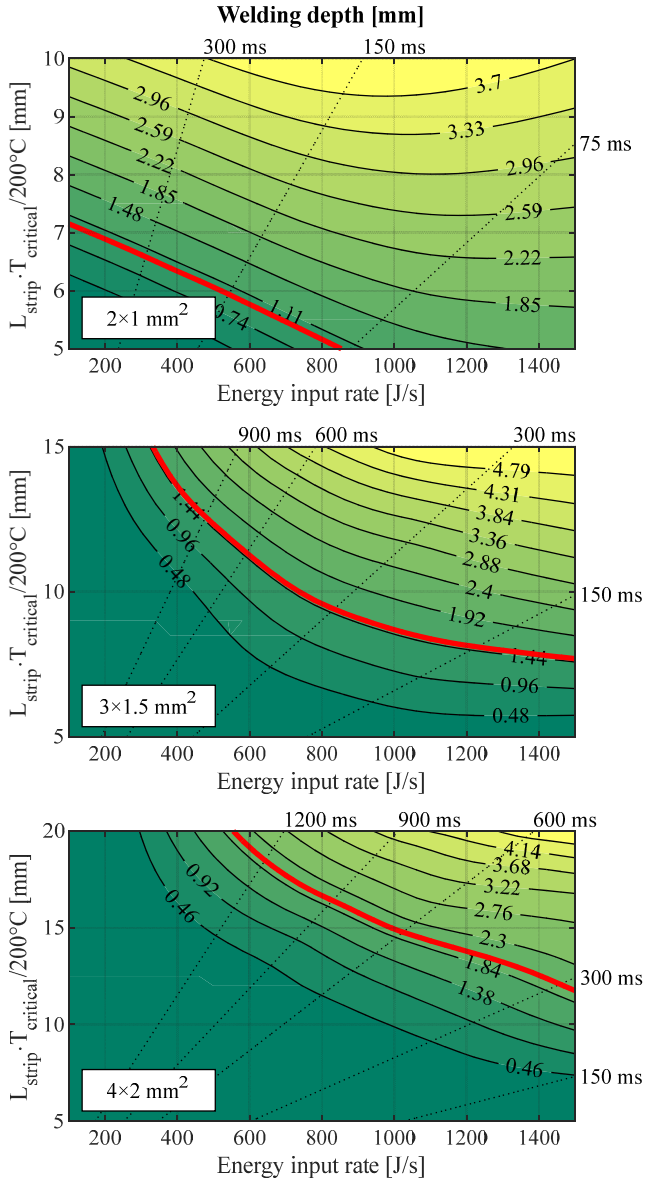

Fig. 9. Welding depths for variations of the energy input rate, welding time and stripping lengths considering a critical temperature of 200°C for wires with cross-sections of 2×1, 3×1.5 and 4×2 mm².

7. Summary and Outlook

The rising importance of electric mobility currently requires the design and production of high-performance traction drives in shortest time and large quantities. This poses high economic risks due to significant coherences between product features and production processes in stator manufacturing. The presented simulation techniques demonstrate that production-oriented design of traction drives can be realized in early stages of product design by numerical analyses and dedicated parameter studies. The conducted studies represent only a fraction of possibilities enabled by model-based design and will therefore be investigated in greater depth in future work.

Acknowledgement

This publication is based on research results of the AnStaHa project that is funded by the Ministry of Economic Affairs, Labour and Housing of Baden-Württemberg. Furthermore, the authors acknowledge support by the state of Baden-Württemberg through bwHPC.

References

[1] A. Kampker, K. Kreisköther, M.K. Buning, P. Treichel, J. Theelen, Automotive quality requirements and process capability in the production of electric motors, in: 2017 7th International Electric Drives Production Conference (EDPC), IEEE, Piscataway, NJ, 2017, pp. 1–8.

[2] M. Halwas, L. Hausmann, F. Wirth, J. Fleischer, B. Jux, M. Doppelbauer, Influences of Design and Manufacturing on the Performance of Electric Traction Drives, in: 2020 International Conference on Electrical Machines (ICEM), IEEE, Piscataway, NJ, 2020, pp. 488–494.

[3] F. Wirth, J. Fleischer, Influence of Wire Tolerances on Hairpin Shaping Processes, in: 2019 9th International Electric Drives Production Conference (EDPC), IEEE, Piscataway, NJ, 2019, pp. 1–8.

[4] A. Riedel, M. Masuch, M. Weigelt, T. Glabel, A. Kuhl, S. Reinstein, J. Franke, Challenges of the Hairpin Technology for Production Techniques, in: C.-E. Kim (Ed.), 2018 21th International Conference on Electrical Machines and Systems (ICEMS), IEEE, Piscataway, NJ, 2018, pp. 2471–2476.

[5] T. Glaessel, D.B. Pinhal, M. Masuch, D. Gerling, J. Franke, Manufacturing Influences on the Motor Performance of Traction Drives with Hairpin Winding, in: 2019 9th International Electric Drives Production Conference (EDPC), IEEE, Piscataway, NJ, 2019, pp. 1–8.

[6] Y. Zhao, D. Li, T. Pei, R. Qu, Overview of the Rectangular Wire Windings AC Electrical Machine, CES Transactions on Electrical Machines and Systems 3 (2019) pp. 160–169. https://doi.org/10.30941/CESTEMS.2019.00022.

[7] M. Halwas, F. Sell-Le Blanc, B. Jux, M. Doppelbauer, F. Wirth, L. Hausmann, J. Hofmann, J. Fleischer, Coherences Between Production Technology and Performance of Electric Traction Drives, in: 2019 9th International Electric Drives Production Conference (EDPC), IEEE, Piscataway, NJ, 2019, pp. 1–9.

[8] M. Weigelt, A. Riedel, M. Masuch, A. Mahr, T. Gläßel, J. Franke, Potentials of an explicit finite element analysis of the bending processes for coated copper wires, in: 2017 7th International Electric Drives Production Conference (EDPC), IEEE, Piscataway, NJ, 2017, pp. 1–5.

[9] F. Wirth, C. Nguyen, J. Hofmann, J. Fleischer, Characterization of Rectangular Copper Wire Forming Properties and Derivation of Control Concepts for the Kinematic Bending of Hairpin Coils, Procedia Manufacturing 47 (2020) , pp. 678–685. https://doi.org/10.1016/j.promfg.2020.04.209.

[10] T. Gläßel, Prozessketten zum Laserstrahlschweißen von flachleiterbasierten Formspulenwicklungen für automobile Traktionsantriebe. PhD dissertation, Erlangen-Nürnberg, 2020.

[11] L. Hausmann, F. Wirth, J. Fleischer, Opportunities of Model-Based Production-Oriented Design of Stators with Hairpin Winding, in: 2020 10th International Electric Drives Production Conference (EDPC), IEEE, Piscataway, NJ, 2020, pp. 1–8, in press.

[12] A. Blom, P. Dunias, P. van Engen, W. Hoving, J. de Kramer, Process spread reduction of laser microspot welding of thin copper parts using real-time control, in: A. Pique, K. Sugioka, P.R. Herman, J. Fieret, F.G. Bachmann, J.J. Dubowski, W. Hoving, K. Washio, D.B. Geohegan, F. Traeger, K. Murakami (Eds.), Photon Processing in Microelectronics and Photonics II, SPIE, 2003, p. 493.